# A New Current-fed Inductive Wireless Charging Transmitter for Large-scale EV In-motion Wireless Charging Infrastructure

# Mckay Waite

Electrical and Computer Engineering
Utah State University
Logan, Utah, USA
mckay.waite@usu.edu

## Regan Zane

Electrical and Computer Engineering
Utah State University
Logan, Utah, USA
regan.zane@usu.edu

## Hongjie Wang

Electrical and Computer Engineering
Utah State University
Logan, Utah, USA
hongjie.wang@usu.edu

Abstract—Large-scale in-motion inductive wireless charging infrastructure could be a key enabler for widespread adoption of electric vehicles (EVs) leading to net-zero carbon emissions for the transportation sector. However, the challenge of distributing power to the numerous transmitters in such large-scale systems has not been adequately investigated. This paper presents further development of a patented novel power distribution architecture that provides improved system efficiency, reliability, and cost in large-scale EV in-motion wireless charging systems. This paper provides details on operation and analysis of the proposed current-fed wireless charging transmitter. The proposed transmitter achieves load-independent transmitter coil current and high tolerance to mistuning. Simulation results from a 1 kW current-fed transmitter design validate the proposed design and analysis.

Index Terms—electric vehicle, in-motion, wireless power transfer, dynamic charging, large-scale, electrified transportation, current-fed

#### I. Introduction

According to a recent study, global electric vehicle (EV) sales supremacy will arrive by 2030, three years earlier than previously expected [1]. As EV adoption accelerates, charging infrastructure is expected to be the main limiting factor over the next decade and beyond [2]. Most efforts to improve EV charging technology have been put into charger development, including wired and wireless chargers, to push for higher power and efficiency, new power converter topologies, and the application of new semiconductor devices [3]–[10]. However, another problem, which has not been adequately addressed, is how to distribute power to the input terminals of the chargers, especially in large-scale scenarios.

The existing power distribution approaches are based on low-voltage dc distribution or grid-frequency ac distribution and focus predominantly on small-scale or pilot application scenarios. These existing system architectures for EV charging

This work is based in part upon work supported by the National Science Foundation through the CAREER Award under Grant No. 204850 and the ASPIRE Engineering Research Center under Grant No. EEC-1941524. Any opinions, findings, and conclusions or recommendations expressed in this material are those of the author(s) and do not necessarily reflect the views of the National Science Foundation.

cannot realize large-scale power distribution to the charger inputs with acceptable performance due to voltage drop in cables, complexity in system wiring, and cost.

One example of a large-scale power distribution network is a dynamic inductive wireless power transfer (DWPT) system designed to charge EVs while the vehicles move on a roadway. DWPT systems can help lower the cost of EVs by reducing the size of the battery, the most expensive part in an EV, and address EV range and charging anxiety [11], [12]. Additionally, through use of bidirectional power converters, vehicle-to-grid (V2G) technology could be implemented in DWPT systems. Benefits of V2G technology have been shown in stationary plug-in and wireless charging applications such as helping to stabilize the grid and promoting large-scale integration of

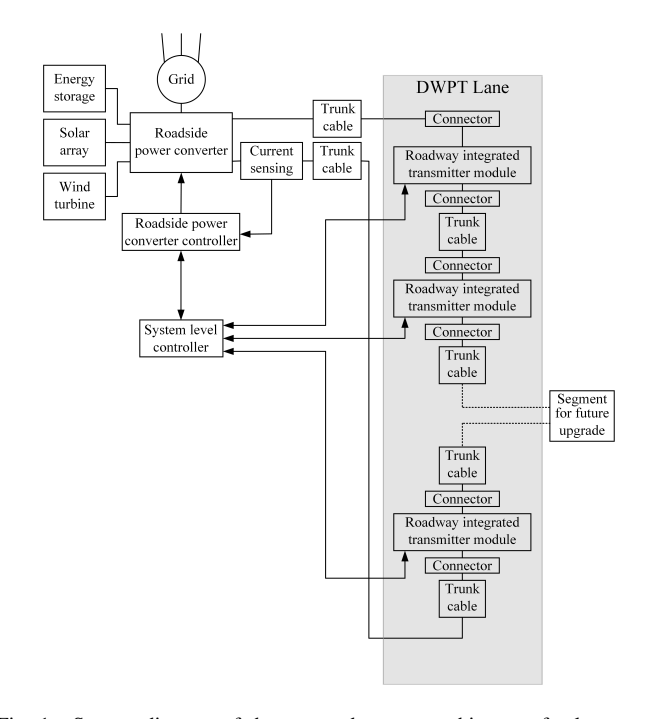


Fig. 1. System diagram of the patented system architecture for large-scale electric vehicle in-motion wireless charging.

renewable energy sources [13]–[15]. Large-scale implementation of DWPT networks also include complications regarding system construction, cost, and efficient power distribution to terminals of the power transmitting units.

To address challenges in power distribution and improve system efficiency with reduced cost for the large-scale EV inmotion wireless charging infrastructure, a new dynamic inductive wireless power transfer system with a power transmitter module has been presented in recently granted patents [16], [17]. The two patents showed a novel system architecture for distributing power to the charger inputs in large-scale inmotion charging applications with [16] focusing on system architecture and [17] presenting a new set of transmitter topologies that can be used in the proposed system architecture. The patented direct current (dc) power distribution architecture, where transmitters are series connected as shown in Fig. 1, achieves power distribution to numerous transmitters in large-scale EV in-motion wireless charging systems with high efficiency, high reliability, and low-cost.

In [18], the authors presented modeling and comparative analysis of different system architectures for large-scale EV inmotion wireless charging systems and validated the benefits of the patented power distribution architecture through modeling and analysis. The key contribution of this paper is the proposal of a new current-fed wireless charging transmitter that is capable of no-load operation, has load independent transmitter coil current, has low component stress, and has high tolerance to component mistuning, which improves the system reliability and performance. Furthermore, the new charging transmitter can be designed to be capable of either unidirectional or bidirectional power flow.

The remainder of this paper is organized as follows. The patents are reviewed in Section II. Section III presents the proposed new current-fed wireless charging transmitter design with detailed analysis. Section IV provides Matlab/PLECS simulation results for a 1 kW transmitter design with 4.43 A transmitter coil current to validate the proposed design and analysis, while conclusion is drawn in Section V.

#### II. REVIEW OF THE PATENTS

As shown in Fig. 1, the patented dc power distribution system architecture has all EV in-motion wireless charging transmitter units connected in series through a trunk cable powered by a roadside power converter with regulated distribution current [16], [17]. The patented system architecture allows a relatively low current to flow through the cables, which results in lower cable losses and allows the use of thinner cables. The large-scale EV in-motion wireless charging system is expected to be pavement integrated with the roadway. For a single-lane scenario, all transmitter units are located in the forward current path and the return current cable sits at ground potential without any cuts, as seen in Fig. 1. For a two-lane scenario, one lane is on the forward current path while the other is on the return current path so that the distribution cables can be fully utilized, as presented in [18]. In the patented system architecture, all pavement integrated transmitter units

need only two connectors for the series connection. The transmitter units are fed from a distribution current regulated by the roadside power converter. The roadside power converter is the interface to utility grid, renewable energy sources, and energy storage, and is capable of eliminating the peak power demand to utility grid caused by the in-motion charging load. With these features and benefits, the patented power distribution architecture can achieve reduced system cost and complexity of construction.

In [17], a dc constant input current driven wireless power transmitter has been patented for the unique power distribution system. The patented transmitter design includes a LC filter at the input, a current-fed H-bridge, and a parallel compensation network for the transmitter coil self-inductance. The patent also presents various hardware sharing configurations to illustrate designs and approaches for reducing system cost.

# III. NEW CURRENT-FED WIRELESS CHARGING TRANSMITTER

In this paper, a new single-stage current-fed H-bridge with CLC compensation transmitter topology, as shown in Fig. 2, for large-scale EV in-motion wireless charging to achieve load-independent transmitter coil current, high tolerance on variation of components' value, and misalignment is proposed. In Fig. 2,  $I_{in}$  is the system distribution current regulated by the roadside power converter,  $C_{in}$  and  $L_{in}$  together is the input filter to achieve expected input voltage ripple,  $Q_{11}$  -  $Q_{42}$ are the MOSFETS for the current-fed H-bridge to generate square current waveform at the H-bridge output,  $i_T$  is the transmitter coil current,  $C_p$ ,  $L_p$ , and  $C_s$  are the components of the proposed compensation network,  $L_T$  represents the transmitter coil self-inductance, and  $R_L$  is the reflected load resistance. As shown in Fig. 2, it has 8 MOSFETs instead of 4 MOSFETs that a voltage-fed H-bridge has. Even with more semiconductor devices, the system cost will still be lower due to the benefits of using low-current rating cables and much-reduced construction complexity, especially for largescale applications. In addition, 4 out of the 8 MOSFETs shown in Fig. 2 can be replaced by diodes if a bi-directional operation is not required to reduce cost and complexity.

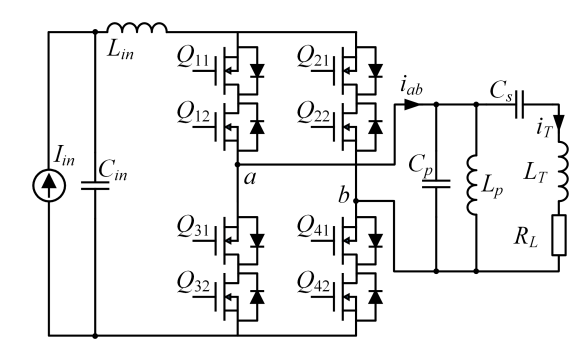


Fig. 2. Circuit topology of the proposed current-fed wireless charging transmitter.

The focus of this paper is the new transmitter topology design and analysis, so the load has been assumed to be a

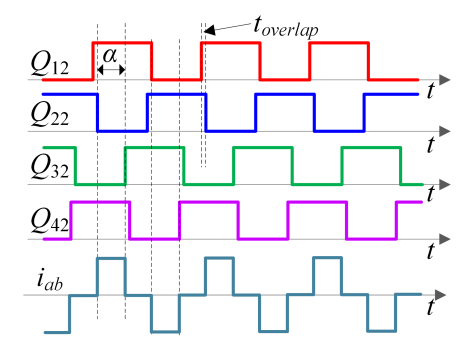


Fig. 3. Phase shift modulation diagram for the proposed current-fed wireless charging transmitter.

resistive load reflected from the receiver side. In this work, phase shift modulation control has been used. Applying the fundamental harmonics approximation analysis to the proposed transmitter topology shown in Fig. 2, the root mean square (rms) value of the transmitter coil current  $i_{T\_rms}$  can be derived as

$$i_{T\_rms} = \frac{2\sqrt{2}I_{in}\sin\left(\frac{\alpha}{2}\right)}{\pi}\frac{\omega^2 L_p C_s}{\sqrt{X}},\tag{1}$$

where,

$$X = (1 - \omega^{2} (L_{T}C_{s} + L_{p}C_{p} + C_{s}L_{p}) + \omega^{4} L_{T}C_{s}L_{p}C_{p})^{2} + (\omega R_{L}(C_{s} - \omega^{2}C_{s}L_{p}C_{p}))^{2}.$$
(2)

In (1) and (2),  $I_{in}$  is the distribution current,  $L_p$ ,  $C_p$ , and  $C_s$  are the passive components in this high-order compensation circuit design,  $L_T$  is the transmitter coil self-inductance, and  $\alpha$  is the phase shift of the current-fed H-bridge ranging from  $0^{\circ}$  to  $180^{\circ}$ . As shown in Fig. 3, the phase shift  $\alpha$  is defined as the phase difference between the top two and bottom two switches. Additionally, there is an overlapping time between the top two switches and between the bottom two switches in each leg, which is different from the voltage-fed H-bridge. The transmitter H-bridge is current-fed, so the overlapping time prevents the occurrence of an open circuit during the switching cycle. In Fig. 3,  $Q_{11}$ ,  $Q_{21}$ ,  $Q_{31}$ , and  $Q_{41}$  are controlled to behave as diodes.

The two resonant frequencies in the CLC compensation circuit are defined as

$$f_{o1} = \frac{1}{2\pi\sqrt{L_p C_p}},\tag{3}$$

$$f_{o2} = \frac{1}{2\pi\sqrt{L_T C_s}}. (4)$$

When  $f_{o1} = f_s$ , the parallel combination of  $L_p$  and  $C_p$ appears as an open circuit at the fundamental switching frequency. Similarly, when  $f_{o2} = f_s$ , the series combination of  $L_T$  and  $C_s$  appears as a short circuit at the fundamental switching frequency. When  $f_{o1} = f_{o2} = f_s$ , from (1) and (2), the transmitter coil current  $i_{T\_rms}$  can be expressed as

$$i_{T\_rms} = \frac{2\sqrt{2}I_{in}\sin\left(\frac{\alpha}{2}\right)}{\pi}.$$
 (5)

From (5), it can be seen that the transmitter coil rms current is independent of load, which means the transmitter side control effort is minimal and could allow the receiver side to control power transfer without real-time communication with the transmitter side. This feature can significantly increase safety, reliability, and robustness of the system.

With the transmitter coil rms current shown in (5), the voltage and current of the components in the compensation circuit can be derived as

$$V_{C_s\_peak} = \sqrt{2}i_{T\_rms}\omega L_T = \frac{\sqrt{2}i_{T\_rms}}{\omega C_s}.$$
 (6)

$$V_{C_{p\_peak}} = \sqrt{2}i_{T\_rms}R_L = \frac{\sqrt{2}P}{i_{T\_rms}},$$
 (7)

$$i_{L_p\_rms} = \frac{i_{T\_rms}R_L}{\omega L_p} = \frac{P}{\omega L_p i_{T\_rms}},$$
 (8)

where P is the power transferred to the receiver side. From (6), it can be seen that the series compensation capacitor voltage is independent from the load. However, not all voltages and currents in the system are independent of load. From (7) and (8), it can be seen that the  $V_{C_{p\_peak}}$  and  $i_{L_{p\_rms}}$  are proportional to the transferred power P.

The value of  $V_{C_p}$  is of particular interest in this topology because  $V_{C_p}$  is the voltage that appears across the devices in the H-bridge. Therefore, to prevent device damage, the selected switching devices must have a sufficient voltage rating to withstand  $V_{C_{n\_peak}}$ . Additionally, the value of  $i_{L_{n\_rms}}$ allows for calculation of the power dissipated in the ESR of the parallel inductor  $L_p$ .

#### IV. SIMULATION AND DISCUSSION

A Matlab/PLECS simulation model of a 1 kW current-fed transmitter design for EV in-motion wireless charging has been developed, as shown in Fig. 4. The equivalent series resistance (ESR) is assumed to be 10 m $\Omega$  for both the input filter capacitor and inductor. The resistor  $R_4$  is a 1 m $\Omega$  sensing resistor for the H-bridge output current  $(i_{ab})$  sensing, and  $R_L$ is the reflected load resistance. In this work, a variable load resistance profile is used to emulate an EV driving through the transmitter coil with 1 kW rated charging power. The parameters of the designed 1 kW current-fed transmitter are tabulated in Table I. The transmitter coil self-inductance is from Ansys simulation of the coil design.

The simulation results of an EV driving through the 1 kW wireless charging transmitter are provided in Fig. 5. From Fig. 5, it can be seen that the input voltage  $V_{in}$  varies proportionally to the power transmitted as the EV drives through the transmitter coil. Similarly, the parallel compensation capacitor voltage  $V_{C_p}$  and the parallel compensation inductor current  $i_{L_p}$  are proportional to the power that is being transferred.

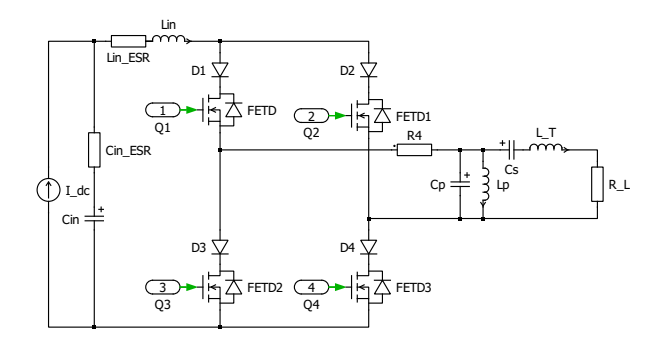


Fig. 4. PLECS simulation model of a 1 kW current-fed transmitter design.

TABLE I PARAMETERS OF THE DESIGNED 1 KW CURRENT-FED TRANSMITTER

Parameter	Theoretical Value	
Power rating P	1 kW	
Switching frequency $f_s$	85 kHz	
Distribution current $I_{dc}$	5 A	
Transmitter coil rms current $i_{T\_rms}$	4.43 A	
Transmitter coil self-inductance $L_T$	$23.2~\mu H$	
Series compensation capacitor $C_s$	$0.15~\mu F$	
Parallel compensation inductor $L_p$	$56.89~\mu H$	
Parallel compensation capacitor $C_p$	$0.06~\mu F$	
Input filter capacitor $C_{in}$	$20~\mu F$	
Input filter inductor $L_{in}$	$500~\mu H$	
Phase shift angle $\alpha$	160°	
·		

The transmitter coil current  $i_T$  and series compensation capacitor voltage  $V_{C_s}$  remain constant throughout the simulation showing they are independent from the load. The steady state waveforms of the proposed transmitter at different operating points are shown in Fig. 6, where Fig. 6(a) is for the 1 kW power transfer operation and Fig. 6(b) is for the no load operation. Some distortion appears in the  $i_T$  no-load waveform due to the presence of switching harmonics. To evaluate the effect of the harmonics on  $i_{T\_rms}$ , the percent deviation (PD) can be examined. The PD is calculated by

$$PD = 100 \cdot \frac{i_{T\_rms\_actual} - i_{T\_rms}}{i_{T\_rms}},$$
 (9)

where  $i_{T\_rms}$  is the theoretical value of the transmitter pad rms current as given by (5) and  $i_{t\_rms\_actual}$  is the actual transmitter pad rms current when harmonics are taken into account. The value for  $i_{t\_rms\_actual}$  is easily obtained through a simulation platform like PLECS. At the no-load operating point,  $i_{T\_rms\_actual} = 4.51$  A. The PD is calculated to be 1.8% using (5) and (9). This small PD shows that the transmitter coil rms current is constant regardless of the power level. The results in Fig. 5 and Fig. 6 validate that the proposed new current-fed transmitter has load independent coil current and operates without the receiver side.

For large-scale EV in-motion wireless charging application, tolerance to mistuning is critical due to nonidealities, manufacturing tolerance, and other factors. Simulation results are

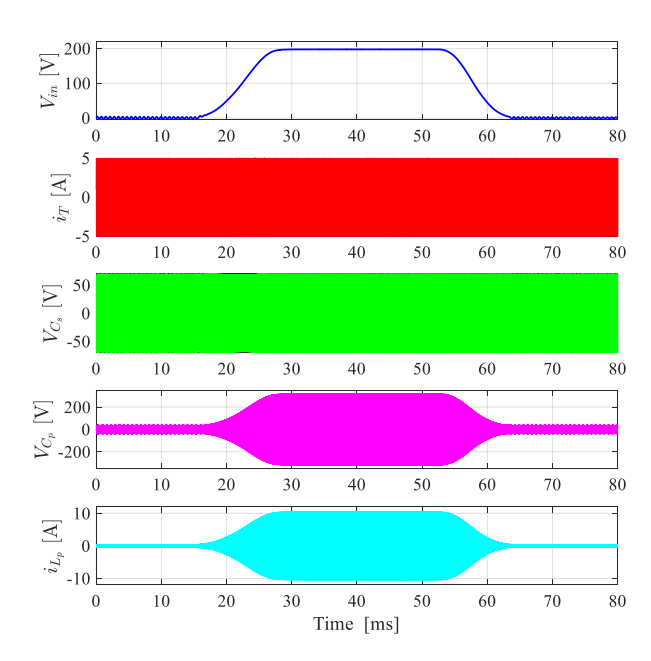


Fig. 5. Simulation results of an electric vehicle driving through the 1 kW wireless charging transmitter.

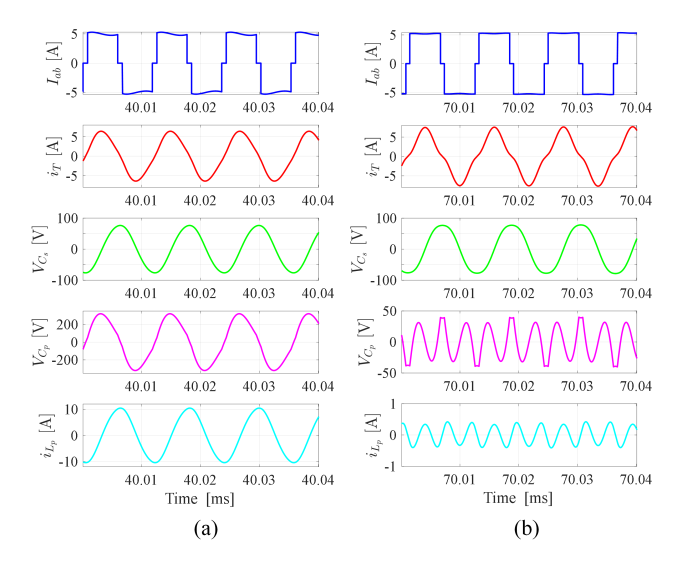


Fig. 6. Steady state waveforms at different operating points. (a) 1 kW power transfer. (b) No-load operation.

provided to validate the high tolerance to mistuning of the proposed current-fed transmitter design, as shown in Fig. 7, where (a) and (b) are the 1 kW and no-load operation results with  $L_T$  being 20% higher and  $L_p$  being 10% higher, and (c) and (d) are the 1 kW and no-load operation results with  $L_T$  being 20% lower and  $L_p$  being 10% lower. From Fig. 7, it can be seen that the proposed transmitter operates properly and tolerates the mistuning introduced by the large variations in the values of the inductors for both full power and no-load operating conditions. More detail about the mistuning tolerance of the transmitter is given in Table II where PD is

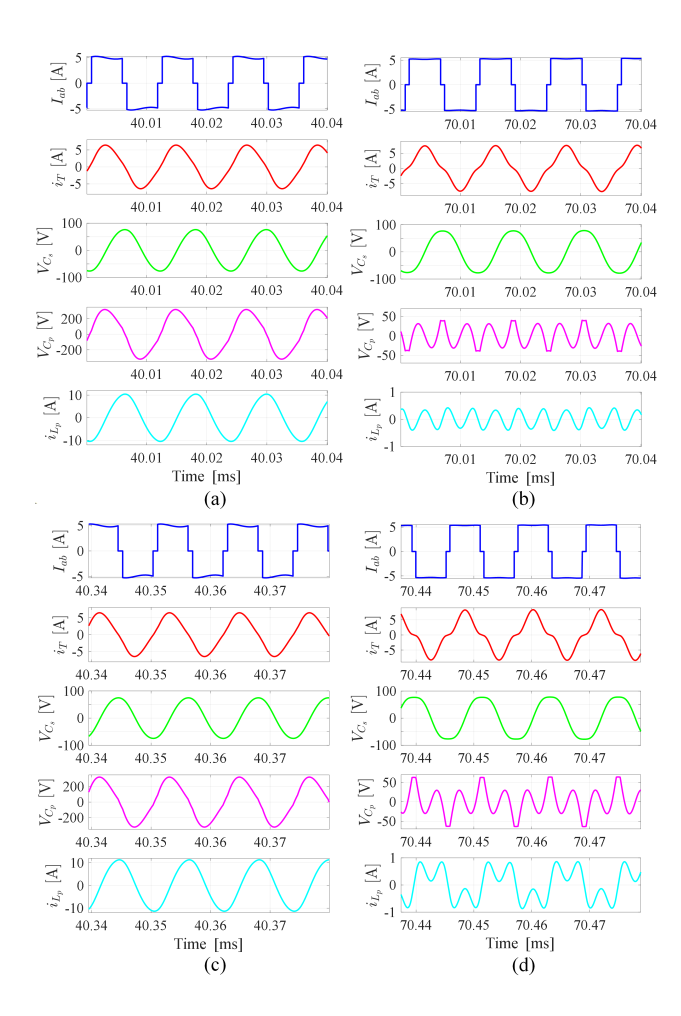


Fig. 7. Steady state waveforms at different operating points with mistuning. (a) 120 kW with coil self-inductance  $L_T$  20% higher and parallel compensation inductance  $L_p$  10% higher. (b) No-load with coil self-inductance  $L_T$  20% higher and parallel compensation inductance  $L_p$  10% higher. (c) 120 kW with coil self-inductance  $L_T$  20% lower and parallel compensation inductance  $L_p$  10% lower. (d) No-load with coil self-inductance  $L_T$  20% lower and parallel compensation inductance  $L_p$  10% lower.

listed for the different operating points.

In the considered scenarios at full-power, the biggest PD occurs when  $L_T$  is 20% lower and  $L_p$  is 10% lower. In this case, the transmitter coil current  $i_{T\_rms\_actual}$  is load independent with a rms value 1.8% higher than  $i_{T\_rms}$ , which means the power transferring capability increases by 3.6%, as shown in Fig. 7(c) and Fig. 7(d). The  $V_{C_s}$ ,  $V_{C_p}$ , and  $i_{L_p}$  increase consequently, but with acceptable values. This change in power transfer can be easily addressed by reducing the phase shift angle  $\alpha$ , and expected operation of the system can be obtained with closed loop control.

#### V. CONCLUSION

A new current-fed wireless charging transmitter has been proposed in this paper as a further development of a patented novel power distribution architecture to achieve improved system efficiency, reliability, and cost for delivering power to the inputs of transmitters in large-scale EV in-motion

 $\begin{tabular}{ll} TABLE \ II \\ TRANSMITTING PAD RMS CURRENT AT DIFFERENT OPERATING POINTS. \\ \end{tabular}$ 

Operating Point	i <sub>T_rms_actual</sub> [A]	PD (%)
No Mistuning (Full Power)	4.40	-0.7
No Mistuning (No Load)	4.51	1.8
$L_T$ 20% $\uparrow$ , $L_p$ 10% $\uparrow$ (Full Power)	4.40	-0.7
$L_T$ 20% $\uparrow$ , $L_p$ 10% $\uparrow$ (No Load)	4.47	0.9
$L_T$ 20% $\downarrow$ , $L_p$ 10% $\downarrow$ (Full Power)	4.35	-1.8
$L_T$ 20% $\downarrow$ , $L_p$ 10% $\downarrow$ (No Load)	4.62	4.3

wireless charging systems. The detailed operation and analysis of the proposed transmitter design has been presented. Matlab/PLECS simulation results from a 1 kW system design have been provided for both tuned and mistuned scenarios to validate the proposed design in terms of the load-independent transmitter coil current operation, high tolerance on the variation of components' value, and robustness to mistuning.

#### REFERENCES

- "Electric vehicles continue charge toward sales dominance ey analysis," https://www.ey.com/en\_gl/news/2023/01/electric-vehicles-continue-charge-toward-sales-dominance-ey-analysis, Jan 2023, (accessed Mar. 8, 2024).
- [2] H. Engel, R. Hensley, S. Knupfer, and S. Sahdev, "Charging ahead: Electric-vehicle infrastructure demand – the basics of charging infrastructure," https://www.mckinsey.com/industries/automotive-andassembly/our-insights/charging-ahead-electric-vehicle-infrastructuredemand, August 2018, (accessed Mar. 8, 2024).
- [3] S. Y. Choi, B. W. Gu, S. Y. Jeong, and C. T. Rim, "Advances in wireless power transfer systems for roadway-powered electric vehicles," *IEEE Journal of Emerging and Selected Topics in Power Electronics*, vol. 3, no. 1, pp. 18–36, 2015.
- [4] H. Tu, H. Feng, S. Srdic, and S. Lukic, "Extreme fast charging of electric vehicles: A technology overview," *IEEE Transactions on Transportation Electrification*, vol. 5, no. 4, pp. 861–878, 2019.
- [5] S. Li and C. C. Mi, "Wireless power transfer for electric vehicle applications," *IEEE Journal of Emerging and Selected Topics in Power Electronics*, vol. 3, no. 1, pp. 4–17, 2015.
- [6] Z. Bi, T. Kan, C. C. Mi, Y. Zhang, Z. Zhao, and G. A. Keoleian, "A review of wireless power transfer for electric vehicles: Prospects to enhance sustainable mobility," *Applied Energy*, vol. 179, pp. 413–425, 2016. [Online]. Available: https://www.sciencedirect.com/science/article/pii/S0306261916309448
- [7] R. Zeng, V. P. Galigekere, O. C. Onar, and B. Ozpineci, "Grid integration and impact analysis of high-power dynamic wireless charging system in distribution network," *IEEE Access*, vol. 9, pp. 6746–6755, 2021.
- [8] F. Jin, A. Nabih, C. Chen, X. Chen, Q. Li, and F. C. Lee, "A high efficiency high density dc/dc converter for battery charger applications," in 2021 IEEE Applied Power Electronics Conference and Exposition (APEC), 2021, pp. 1767–1774.
- [9] D. Chou, Z. Liao, K. Fernandez, T. Gebrael, G. Popovic, R. Mahony, N. Miljkovic, and R. C. N. Pilawa-Podgurski, "An interleaved 6-level gan bidirectional converter with an active energy buffer for level ii electric vehicle charging," in 2021 IEEE Applied Power Electronics Conference and Exposition (APEC), 2021, pp. 1203–1208.
- [10] L. Zhu, H. Bai, A. Brown, and L. Keuck, "A current-fed three-port dc/dc converter for integration of on-board charger and auxiliary power module in electric vehicles," in 2021 IEEE Applied Power Electronics Conference and Exposition (APEC), 2021, pp. 577–582.
- [11] M. Chinthavali and O. C. Onar, "Tutorial on wireless power transfer systems," in 2016 IEEE Transportation Electrification Conference and Expo (ITEC), 2016, pp. 1–142.
- [12] S. Lukic and Z. Pantic, "Cutting the cord: Static and dynamic inductive wireless charging of electric vehicles," *IEEE Electrification Magazine*, vol. 1, no. 1, pp. 57–64, 2013.

[13] D. Patil, M. K. McDonough, J. M. Miller, B. Fahimi, and P. T. Balsara, "Wireless power transfer for vehicular applications: Overview and challenges," *IEEE Transactions on Transportation Electrification*, vol. 4, no. 1, pp. 3–37, 2018.

- [14] W. Kempton and J. Tomić, "Vehicle-to-grid power implementation: From stabilizing the grid to supporting large-scale renewable energy," *Journal of Power Sources*, vol. 144, no. 1, pp. 280–294, 2005. [Online]. Available: https://www.sciencedirect.com/science/article/pii/S0378775305000212
- [15] U. K. Madawala and D. J. Thrimawithana, "A bidirectional inductive power interface for electric vehicles in v2g systems," *IEEE Transactions* on *Industrial Electronics*, vol. 58, no. 10, pp. 4789–4796, 2011.
- [16] H. Wang and R. Zane, "Dynamic inductive wireless power transmitter system with a power transmitter module," U.S. Patent 11 059 380 B2, Jul. 1, 2021.
- [17] —, "Dynamic inductive wireless power transmitter system with a power transmitter module," U.S. Patent 10 727 693 B2, Jul. 28, 2020.
- [18] M. Chawla, A. Zade, T. Newbolt, P. Mandal, A. Kamineni, H. Wang, and R. Zane, "Modeling and comparative analysis of power distribution architectures for large-scale electric vehicle in-motion wireless charging infrastructures," in 2022 Wireless Power Week (WPW), 2022, pp. 887–892.